Fragmentation of Neutron Star Matter

P. N. Alcain and C. O. Dorso
Departamento de Física, FCEyN, UBA and IFIBA, Conicet, Pabellón 1, Ciudad Universitaria, 1428 Buenos Aires, Argentina and IFIBA-CONICET
(Dated: January 28, 2016)

Background: Neutron stars are astronomical systems with nucleons submitted to extreme conditions. Due to the long range coulomb repulsion between protons, the system has structural inhomogeneities. These structural inhomogeneities arise also in expanding systems, where the fragment distribution is highly dependent on the thermodynamical conditions (temperature, proton fraction, ...) and the expansion velocity.

Purpose: We aim to find the different regimes of fragment distribution, and the existence of infinite clusters.

Method: We study the dynamics of the nucleons with a semiclassical molecular dynamics model. Starting with an equilibrium configuration, we expand the system homgeneously until we arrive to an asymptotical configuration (i. e. very low final densities). We study the fragment distribution throughout this expansion.

Results: We found the typical regimes of the asymptotical fragment distribution of an expansion: u-shaped, power law and exponential. Another key feature in our calculations is that, since the interaction between protons is long range repulsive, we do not have always an infinite fragment. We found that, as expected, the faster the expansion velocity is, the quicker the infinite fragment disappears.

Conclusions: We have developed a graph-based tool for the identification of infinite fragments, and found a transition from U-shaped to exponential fragment mass distribution with increasing expansion rate.

PACS numbers: PACS 24.10.Lx, 02.70.Ns, 26.60.Gj, 21.30.Fe

I. INTRODUCTION

A neutron star is an astronomical object with a radius of approximately 10 km and a mass of about $m \simeq 1.5 M_\odot$. Its structure can be divided in two parts, according to current models [1, 2]: the *crust*, about 1.5 km thick and with a density of up to half the normal nuclear density ρ_0; and the *core*, where the structure is still unknown and remains highly speculative [3]. Ravenhall *et al.* in Ref. [4] and Hashimoto *et al.* in Ref. [5] proposed that the neutron star crust is composed by the structures known as *nuclear pasta*.

When two neutron stars collide, a neutron star merger happens. According to hydrodynamic models [6], these have typical expansions coefficents of $\eta = 10^{-21}\,\mathrm{c/fm} < \eta < 4 \cdot 10^{-20}\,\mathrm{c/fm}$.

Semiclassical models with molecular dynamics have been used to study the *nuclear pasta* regime, with mainly two parametrizations of the interaction: Simple Semiclassical Potential [7], Quantum Molecular Dynamics [8] and Classical Molecular Dynamics [9, 10].

Multifragmentation in nuclear systems has been studied before [11, 12], but mostly with nuclear matter (without Coulomb interaction). In a recent work by Caplan et al [13], expanding neutron star matter has been studied as possible explanations for nucleosynthesis in neutron star mergers.

Inspired by the neutron star merger, we perform a study on the fragmentation of expanding neutron star matter. In section II we define the model we use and in section III we explain how we simulate the expansion of the system. To analyze fragments, we describe in section IV the cluster recognition algorithm, with emphasis on the identification of infinite fragments.

II. CLASSICAL MOLECULAR DYNAMICS

In this work, we study fragmentation of Neutron Star Matter under pasta-like conditions with the classical molecular dynamics model CMD. It has been used in several heavy-ion reaction studies to: help understand experimental data [14]; identify phase-transition signals and other critical phenomena [15–19]; and explore the caloric curve [20] and isoscaling [21, 22]. CMD uses two two-body potentials to describe the interaction of nucleons, which are a combination of Yukawa potentials:

$$V_{np}^{\mathrm{CMD}}(r) = v_r \exp(-\mu_r r)/r - v_a \exp(-\mu_a r)/r$$
$$V_{nn}^{\mathrm{CMD}}(r) = v_0 \exp(-\mu_0 r)/r$$

where V_{np} is the potential between a neutron and a proton, and V_{nn} is the repulsive interaction between either nn or pp. The cutoff radius is $r_c = 5.4\,\mathrm{fm}$ and for $r > r_c$ both potentials are set to zero. The Yukawa parameters μ_r, μ_a and μ_0 were determined to yield an equilibrium density of $\rho_0 = 0.16\,\mathrm{fm}^{-3}$, a binding energy $E(\rho_0) = 16\,\mathrm{MeV/nucleon}$ and a compressibility of $250\,\mathrm{MeV}$.

To simulate an infinite medium, we used this potential with $N = 11000$ particles under periodic boundary conditions, with different proton fraction (i.e. with $x = Z/A = 0.2 < x < 0.4$) in cubical boxes with sizes adjusted to have densities $\rho = 0.05\,\mathrm{fm}^{-3}$ and $\rho = 0.08\,\mathrm{fm}^{-3}$. These simulations have been done with LAMMPS [23], using its GPU package [24].

A. Coulomb interaction in the model

Since a neutralizing electron gas embeds the nucleons in the neutron star crust, the Coulomb forces among protons are screened. The model we used to model this screening effect is the Thomas-Fermi approximation, used with various nuclear models [8, 9, 25]. According to this approximation, protons interact via a Yukawa-like potential, with a screening length λ:

$$V_{TF}(r) = q^2 \frac{e^{-r/\lambda}}{r}.$$

Theoretical estimates for the screening length λ are $\lambda \sim 100\,\mathrm{fm}$ [26], but we set the screening length to $\lambda = 20\,\mathrm{fm}$. This choice was based on previous studies [27], where we have shown that this value is enough to adequately reproduce the expected length scale of density fluctuations for this model, while larger screening lengths would be a computational diffculty. We analyze the opacity to neutrinos of the structures for different proton fractions and densities.

III. EXPANSION

To simulate an expanding system we scale linearly with time the length of the box in every dimension,

$$L(t) = L_0(1 + \eta\, t)$$

This, however, is not enough to expand the system collectively. We also need the particles inside the cell to expand like the box. In order to accomplish this, based on Ref. [28], we add to each particle a velocity v_{exp} dependent on the position in the box:

$$\mathbf{v_{exp}} = \eta\, \mathbf{r}$$

We can see from this expression that the particles in the edge of the box will have an expanding velocity equal to that of the box.

Another effect to consider of this expansion is that when a particle crosses a boundary its velocity has to change according to the velocity of the expanding box. For example, if the particle crosses the left-hand boundary of the periodic box, the velocity of the image particle $v_i^\dagger$ on the right-hand must be modified $v_i^\dagger = v_i + L_0\,\eta$.

IV. CLUSTER RECOGNITION

In typical configurations we have not only the structure known as nuclear pasta, but also a nucleon gas that surrounds the nuclear pasta. In order to properly characterize the pasta phases, we must know which particles belong to the pasta phases and which belong to this gas. To do so, we have to find the clusters that are formed along the simulation.

One of the algorithms to identify cluster formation is Minimum Spanning Tree (MST). In MST algorithm, two particles belong to the same cluster $\{C_n^{\mathrm{MST}}\}$ if the relative distance of the particles is less than a cutoff distance r_{cut}:

$$i \in C_n^{\mathrm{MST}} \Leftrightarrow \exists j \in C_n \mid r_{ij} < r_{cut}$$

This cluster definition works correctly for systems with no kinetic energy, and it is based in the attractive tail of the nuclear interaction. However, if the particles have a non-zero temperature, we can have a situation of two particles that are closer than the cutoff radius, but with a large relative kinetic energy.

To deal with situations of non-zero temperatures, we need to take into account the relative momentum among particles. One of the most sophisticated methods to accomplish this is the Early Cluster Recognition Algorithm (ECRA) [29]. In this algorithm, the particles are partitioned in different disjoint clusters C_n^{ECRA}, with the total energy in each cluster:

$$\epsilon_n = \sum_{i \in C_n} K_i^{CM} + \sum_{i,j \in C_n} V_{ij}$$

where K_i^{CM} is the kinetic energy relative to the center of mass of the cluster. The set of clusters $\{C_n\}$ then is the one that minimizes the sum of all the cluster energies $E_{\mathrm{partition}} = \sum_n \epsilon_n$.

ECRA algorithm can be easily used for small systems [30], but being a combinatorial optimization, it cannot be used in large systems. While finding ECRA clusters is very expensive computationally, using simply MST clusters can give extremely biased results towards large clusters. We have decided to go for a middle ground choice, the Minimum Spanning Tree Energy (MSTE) algorithm [9]. This algorithm is a modification of MST, taking into account the kinetic energy. According to MSTE, two particles belong to the same cluster $\{C_n^{\mathrm{MSTE}}\}$ if they are energy bound:

$$i \in C_n^{\mathrm{MSTE}} \Leftrightarrow \exists j \in C_n : V_{ij} + K_{ij} \leq 0$$

While this algorithm doesn't yield the same theoretically sound results from ECRA, it still avoids the largest pitfall of naïve MST implementations for the temperatures used in this work.

A. Infinite Clusters

We developed an algorithm for the recognition of infinite clusters across the boundaries. We explain here in detail the implementation for MST clusters in 2D, being the MSTE and 3D extension straightforward. In figure 1 we see a schematical representation of 2D clusters recognized in a periodic cell, labeled from 1 to 6 (note that these clusters don't connect yet through the periodic walls).

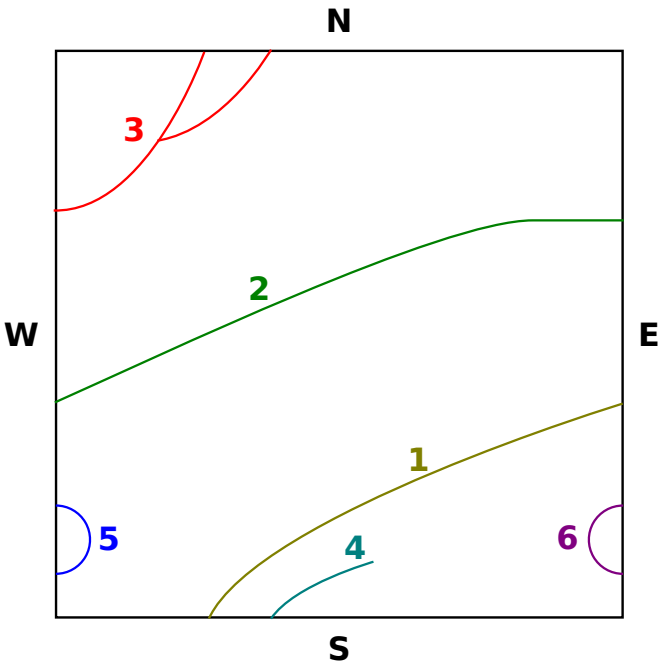

Figure 1: (Color online) Schematical representation of 2D clusters, recognized only in the cell and not through the periodic walls, labeled as N, S, W, E. The clusters inside the cell are labeled from 1 to 6,

In order to find the connections of these clusters through the boundaries, we draw a labeled graph of the clusters, where we connect clusters depending on whether they connect or not through a wall and label such connection with the wall label. For example, we begin with cluster 1. It connects with cluster 2 going out through the E wall, therefore we add a $1 \to 2$ connection labeled as E. Symetrically, we add a $2 \to 1$ connection labeled as W. Now we go for the pair 1-3. It connects going out through the S wall, so we add $1 \to 3$ labeled as S and $3 \to 1$ labeld as N. Cluster 1 does not connect with 4, 5, or 6, therefore those are the only connections we have. Once we've done that, we get the graph of figure 2.

We now wonder whether these subgraphs represent an infinite cluster or not not. In order to have an infinite clusters, we need to have a loop (the opposite is not true: having a loop is not enough to have an infinite cluster, as we can see in subragph 5–6), so we first identify loops and mark them as candidates for infinite clusters. Every connection adds to a loop (since the graph connections are back and forth), but we know from inspecting the figure 2 that the cluster 1–2–3 is infinite. Finding out what makes, in the graph, the cluster 1–2–3 infinite is key to identifiy infinite clusters. And the key feature of cluster 1–2–3 is that its loop 1–2–3–1 can be transversed through the walls E–E–S, while loops like 5–6 can be transversed only through E–W. Now, in order for the cluster to be infinite, we need it to extend infinitely in (at least) one direction. So once we have the list of walls of the loop, we create a magnitude I associated to each loop

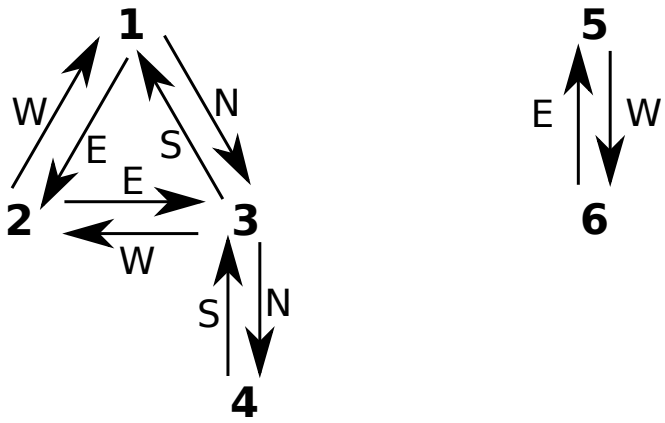

Figure 2: Graph of the clusters with connections labeled by the wall of the boundary they connect through. The graph can be divided in 2 subgraphs that don't connect: 1–2–3–4 and 5–6. Each of these subgraphs is as cluster when periodic boundary conditions are considered.

that is created as follows: beginning with $I = 0$, we add a value M_i if there is (at least one) i wall. The values are: $M_E = 1$, $M_W = -1$, $M_N = 2$, $M_S = -2$. If I is nonzero, then the loop is infinite. For example, for the loop E–E–S, we have E and S walls, so $I = M_E + M_S = 3$ and the loop is infinite. For the loop E–W, $I = M_E + M_W = 0$, and the loop is finite.

V. RESULTS

In figure 3 we show the initial and final states for the expansion of $N = 11000$ particle primordial cell (see caption for details) for the case of low velocity expansion. It can be immediately seen that though the initial configuration shows a compact particle distribution, the final configuration consists of *gnocchi* structures (almost spherical fragments) with a mass of about 80 particles.

In figure 4 we show the fraction of particles in the primordial cell that form part of an infinite cluster (*Infinite Fragment Fraction*, IFF). It can be easily seen that in the early stages of the evolution, due to the fact that the temperature is low, most of the system in the primordial cell belongs to the infinite clusters. But as the system evolves according to the expansion rate as explained above, the IFF goes down and goes to zero rather quickly, meaning that there is no more infinite fragment in the system. See caption for details.

Figure 5 shows the asymptotical fragment mass distribution for 4 different expansion rates. In this case, the MSTE algorithm has been applied over the primordial cell, taking into account periodic boundary conditions knowing that there is no infinite fragment as shown in figure 4. It can be seen that as the homogeneous expansion velocity increases, the fragment mass distribution displays the familiar transition from U-shaped to exponential decay. Somewhere in between, a power law dis-

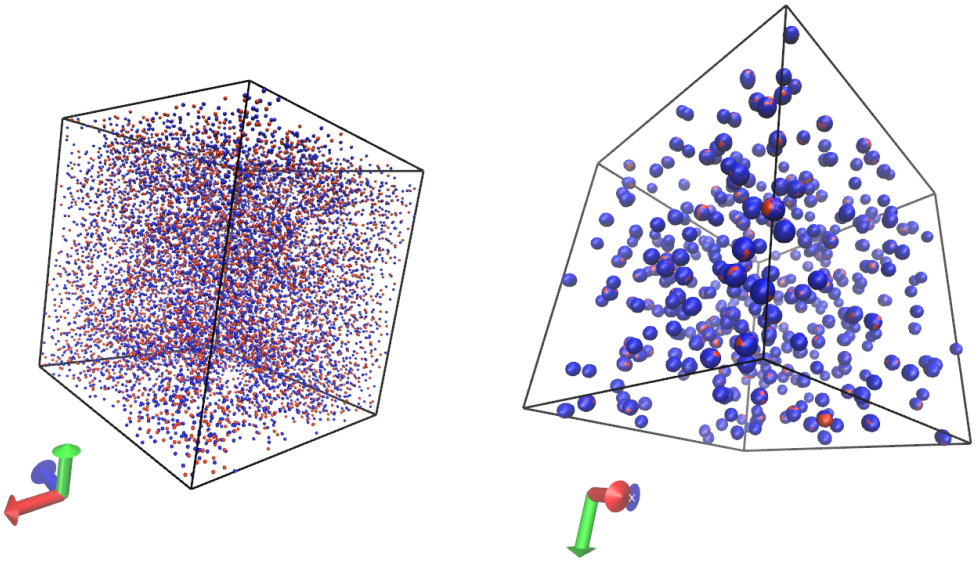

(a) $\eta = 0.0001\,\mathrm{fm/c}$ (b) $\eta = 0.0005\,\mathrm{fm/c}$

Figure 3: (Color online) Snapshots of a system in the initial configuration 3a and the final expanded system 3b. In the expanded system we see clearly formed *gnocchi* clusters

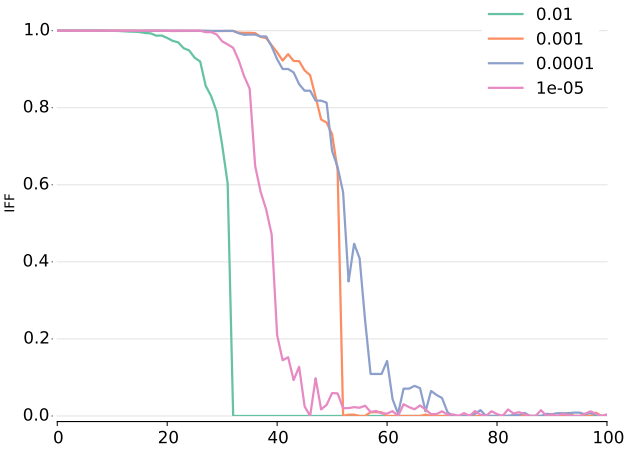

Figure 4: (Color online) Infinite Fragment Fraction (see text) as a function of the length of the edge of the primordial cell. For every expansion rate displayed the IFF goes to zero in the asymptotic regime.

tribution is to be expected. In particular, figure 5c shows that with an expansion of $\eta = 0.009\,\mathrm{fm/c}$ we are close to a power law distribution. It is interesting to note that at variance with percolation or Lennard-Jones systems, due to the presence of the Coulomb long range repulsion term, it is not possible to see an infinite cluster in the asymptotical regime. Moreover, together with the rather large rate of expansion, we do not expect to find big clusters.

VI. DISCUSSION AND CONCLUDING REMARKS

In this work we have performed numerical experiments of homogenously expanding systems with not very small amount of particles in the primordial cell. In order to analyze the fragment structure of such a system as a function of time, we have developed a graph-based tool for the identification of infinite fragments for any definition of percolation-like (i. e., additive) clusters. Once this formalism is applied to the above mentioned simulations, we have been able to identify the region in which a power-law distribution of masses is expected. The fragment mass distribution shapes range from U-like to exponential decay.

We are currently performing simulations with more number of particles to properly characterize the critical behavior of the system.

ACKNOWLEDGMENTS

This work was partially supported by grants from ANPCyT (PICT-2013-1692), CONICET and UBACyT.

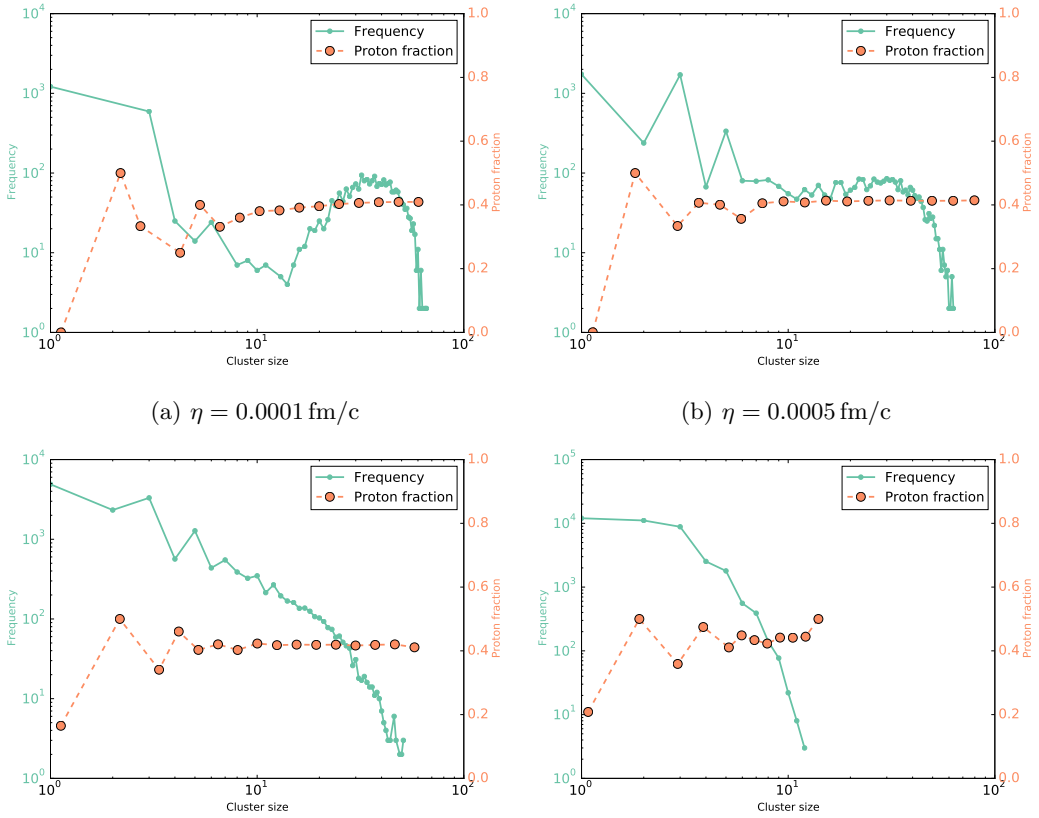

(a) $\eta = 0.0001\,\mathrm{fm/c}$ (b) $\eta = 0.0005\,\mathrm{fm/c}$

(c) $\eta = 0.009\,\mathrm{fm/c}$ (d) $\eta = 0.03\,\mathrm{fm/c}$

Figure 5: (Color online) Fragment mass distribution. Labels grow with larger expansion rates. System consisting of 11000 particles with $x = 0.4$ and initial density $\rho_0 = 0.08\,\mathrm{fm}^{-3}$

[1] D. Page, J. M. Lattimer, M. Prakash, and A. W. Steiner, ApJS **155**, 623 (2004).
[2] U. Geppert, M. Küker, and D. Page, Astronomy & Astrophysics **426**, 11 (2004).
[3] S. Woosley and T. Janka, Nature Physics **1**, 147 (2005).
[4] D. G. Ravenhall, C. J. Pethick, and J. R. Wilson, Phys. Rev. Lett. **50**, 2066 (1983).
[5] M.-a. Hashimoto, H. Seki, and M. Yamada, Prog. Theor. Phys. **71**, 320 (1984).
[6] S. Goriely, A. Bauswein, and H.-T. Janka, ApJ **738**, L32 (2011).
[7] C. Horowitz, M. Pérez-García, J. Carriere, D. Berry, and J. Piekarewicz, Phys. Rev. C **70**, 065806 (2004).
[8] T. Maruyama, K. Niita, K. Oyamatsu, T. Maruyama, S. Chiba, and A. Iwamoto, Phys. Rev. C **57**, 655 (1998).
[9] C. O. Dorso, P. A. Giménez Molinelli, and J. A. López, Phys. Rev. C **86**, 055805 (2012).
[10] P. N. Alcain, P. A. Giménez Molinelli, and C. O. Dorso, Phys. Rev. C **90**, 065803 (2014).
[11] A. Bonasera, M. Bruno, C. O. Dorso, and F. Mastinu, (2000).
[12] S. Chikazumi, T. Maruyama, S. Chiba, K. Niita, and A. Iwamoto, Phys. Rev. C **63**, 024602 (2001).
[13] M. E. Caplan, A. S. Schneider, C. J. Horowitz, and D. K. Berry, Phys. Rev. C **91**, 065802 (2015).
[14] A. Chernomoretz, L. Gingras, Y. Larochelle, L. Beaulieu, R. Roy, C. St-Pierre, and C. O. Dorso, Phys. Rev. C **65**, 054613 (2002).
[15] J. A. López and C. Dorso, *Lectures Notes on Phase Transformations in Nuclear Matter* (WORLD SCIENTIFIC, 2000).
[16] A. Barranon, C. O. Dorso, and J. A. Lopez, Revista mexicana de física **47**, 93 (2001).
[17] C. O. Dorso and J. A. López, Phys. Rev. C **64**, 027602 (2001).
[18] A. Barranón, R. Cárdenas, C. O. Dorso, and J. A. López, APH N.S., Heavy Ion Physics **17**, 59 (2003).
[19] A. Barrañón, C. O. Dorso, and J. A. López, Nuclear Physics A **791**, 222 (2007).
[20] A. Barrañón, J. Roa, and J. López, Phys. Rev. C **69**, 014601 (2004).
[21] C. O. Dorso, C. R. Escudero, M. Ison, and J. A. López, Phys. Rev. C **73**, 044601 (2006).
[22] C. A. Dorso, P. A. G. Molinelli, and J. A. López, J. Phys. G: Nucl. Part. Phys. **38**, 115101 (2011).
[23] S. Plimpton, Journal of Computational Physics **117**, 1 (1995).
[24] W. M. Brown, A. Kohlmeyer, S. J. Plimpton, and A. N.

Tharrington, Computer Physics Communications **183**, 449 (2012).
[25] C. J. Horowitz, M. A. Pérez-García, and J. Piekarewicz, Phys. Rev. C **69**, 045804 (2004).
[26] A. L. Fetter and J. D. Walecka, *Quantum Theory of Many-particle Systems* (Courier Dover Publications, 2003).
[27] P. N. Alcain, P. A. Giménez Molinelli, J. I. Nichols, and C. O. Dorso, Phys. Rev. C **89**, 055801 (2014).
[28] C. O. Dorso and A. Strachan, Phys. Rev. B **54**, 236 (1996).
[29] C. Dorso and J. Randrup, Physics Letters B **301**, 328 (1993).
[30] C. O. Dorso and P. E. Balonga, Phys. Rev. C **50**, 991 (1994).